



ISSN: 2447-3359

REVISTA DE GEOCIÊNCIAS DO NORDESTE

Northeast Geosciences Journal

v. 7, nº 2 (2021)

<https://doi.org/10.21680/2447-3359.2021v7n2ID22034>



ANALYSIS OF PHYSICAL VULNERABILITY INDICES USING GEOTECHNOLOGIES IN THE BARREIRA DO INFERNO REGION OF RIO GRANDE DO NORTE STATE, BRAZIL

Venerando Eustáquio Amaro¹; Ada Cristina Scudelari²; Diego Souza de Oliveira³; Ivens Lorrán Clemente de Lacerda⁴; Maria de Fátima Alves de Matos⁵

¹Geologist, Department of Civil Engineering, Federal University of Rio Grande do Norte (UFRN), Natal, Brazil.

ORCID: <https://orcid.org/0000-0001-7357-2200>

Email: venerando.amaro@gmail.com

²Civil Engineer, Federal University of Rio Grande do Norte (UFRN), Natal, Brazil.

ORCID: <https://orcid.org/0000-0001-7594-1196>

Email: adaufrn@gmail.com

³Civil Engineer, Department of Civil Engineering, Maurício de Uninassau Faculty (UNINASSAU), Natal, Brazil.

ORCID: <https://orcid.org/0000-0002-2700-2917>

Email: diego_s.oliveira@hotmail.com

⁴Civil Engineer, Graduate Civil Engineering Program, Federal University of Rio Grande do Norte (UFRN), Natal, Brazil.

ORCID: <https://orcid.org/0000-0002-1331-2527>

Email: ivenslorran@hotmail.com

⁵Geographer, Graduate Civil Engineering Program, Federal University of Rio Grande do Norte (UFRN), Natal, Brazil.

ORCID: <https://orcid.org/0000-0002-2864-2027>

Email: mfatimaalves.m@gmail.com

Abstract

This study presents the physical vulnerability indices in the Barreira do Inferno region, municipality of Parnamirim, Rio Grande do Norte state (RN), Brazil. The natural (NV) and environmental vulnerability (EV) indices were calculated using weighted statistical analysis of the thematic classes geomorphology, slope, soils, vegetation, geology, land use and cover. The thematic variables were evaluated to reduce subjectivity and dimensionality through Analytical Hierarchy

Process and Principal Component Analysis. The results showed the predominance of intermediate, high and very high vulnerability classes in 75 and 79.1% of the total area on the VN and VA maps, respectively. The Coastal Vulnerability Index (CVI) of erosion was established based on physical and dynamic variables for three different future climate change scenarios projected by the Intergovernmental Panel on Climate Change. In the optimistic scenario, the CVI is low along 100% of the coastline (CL). In the pessimistic projection, 31% of the CL exhibits intermediate vulnerability.

Palavras-chave: Natural Vulnerability; Environmental Vulnerability; CVI; Northeastern Brazil.

ANÁLISE DE ÍNDICES DE VULNERABILIDADE FÍSICA COM USO DE GEOTECHNOLOGIAS NA REGIÃO DA BARREIRA DO INFERNO/RN

Resumo

Este estudo apresenta a determinação de índices de vulnerabilidade física na região da Barreira do Inferno, Município de Parnamirim/RN. Os índices de Vulnerabilidade Natural (VN) e Vulnerabilidade Ambiental (VA) foram calculados por meio da análise estatística ponderada das classes temáticas de geomorfologia, declividade, solos, vegetação, geologia, uso e cobertura do solo. As variáveis temáticas foram avaliadas para redução da subjetividade e da dimensionalidade por meio do Processo Analítico Hierárquico e da Análise por Principais Componentes. Os resultados mostraram o domínio de classes de média, alta e muita alta vulnerabilidade em 75% e 79,1% da área total nos mapas de VN e VA, respectivamente. O Índice de Vulnerabilidade Costeira (IVC) à erosão foi estabelecido a partir de variáveis físicas e dinâmicas para três diferentes cenários futuros de mudanças climáticas do Painel Intergovernamental sobre Mudanças do Clima. O IVC em 100% da linha de costa (LC) é de baixa vulnerabilidade no cenário otimista. Na projeção pessimista 31% da extensão da LC está em vulnerabilidade média.

Keywords: Vulnerabilidade Natural; Vulnerabilidade Ambiental; IVC; Nordeste do Brasil.

ANÁLISIS DE ÍNDICES DE VULNERABILIDAD FÍSICA UTILIZANDO GEOTECNOLOGÍAS EN LA REGIÓN DE BARREIRA DO INFERNO/RN

Resumen

Este estudio presenta la determinación de los índices de vulnerabilidad física en la región de la Barreira do Inferno, Municipio de Parnamirim/RN. Los índices de vulnerabilidad natural (VN) y vulnerabilidad ambiental (VA) se calcularon mediante análisis estadísticos ponderados de las clases temáticas de geomorfología, pendiente, suelos, vegetación, geología, uso del suelo y ocupación. Las variables temáticas se evaluaron para reducir la subjetividad y dimensionalidad a través del Proceso Analítico Jerárquico y el Análisis de Componentes Principales. Los resultados mostraron el dominio de las clases de vulnerabilidad media, alta y muy alta en el 75% y el 79,1% del área total en los mapas VN y VA, respectivamente. El índice de vulnerabilidad costera (IVC) a la erosión se estableció sobre la base de variables físicas y dinámicas para tres escenarios de cambio climático futuros diferentes del Grupo Intergubernamental de Investigación sobre el Cambio Climático. El CIV en el 100% de la costa es de baja vulnerabilidad en el escenario optimista. En la proyección pesimista, el 31% de la extensión de la costa está en vulnerabilidad media.

Palabras-clave: Vulnerabilidad natural; Vulnerabilidad Ambiental; IVC; Nordeste de Brasil.

1. INTRODUCTION

Physical changes on seashores have been increasing due to the growing frequency and intensity of extreme climatic events and the increase in generally disordered demographic density and infrastructure. According to the United Nations (UNDESA, 2017), at least 600 million people, or nearly 10% of the world's population in 2017, live in coastal zones that are less than 10m above sea level and around 2.4 billion, or almost 40% of the population live within 100km of the coastline (CL).

Coastal communities, especially those established in flat morphological domains, are subject to risks and hazards induced by climate change, such as more frequent and intense storms and a rise in relative sea level (RSL) and hydrodynamic forcing energy (MCGRANAHAN *et al.*, 2007). These increasingly frequent episodes heighten the potential exposure of populations, for example, to erosion and coastal flooding, resulting from the synergic combination of factors such as strong winds, high waves and tides and extreme rain events. Likewise, these conditions are a significant threat to coastal ecosystems, since they increase saltwater intrusion into surface and subterranean waters and reduce ecosystems in the humid coastal zones, such as mangrove swamps and restingas (NICHOLLS *et al.*, 2007). Thus, understanding these inter-relationships is essential for coastal planning and management, in addition to helping assess the benefits of early and safe decisions on adaptations to climate influences and the costs of delaying or lack of mitigating actions in the present (KULP *et al.*, 2019).

Given that this geographic unit is especially subject to the complex interactions between the physical variables and socioeconomic factors, the seashore exhibits specific

characteristics along its extension, and distinct vulnerabilities for each stretch of the coast (BUSMAN *et al.*, 2016; BRAGA; PIMENTEL, 2019). The term vulnerability can be described as the set of characteristics of a community, derived from the physical, socioeconomic and environmental variables that determine its ability to anticipate, survive, resist and recover from the impact of natural hazards (KOLLURA, 1996).

Broader studies on coastal vulnerability to erosion and flooding use indices to combine the components of the physical and socioeconomic environment at the regional and local level, in order to understand the relationships between the physical susceptibility of coastal stretches and communities (GORNITZ, 1990; MCLAUGHLIN *et al.* 2002; BORUFF *et al.*, 2005). Another approach is to assess the variables of the natural physical environment, or natural vulnerability (NV) and environmental vulnerability (EV, TAGLIANI, 2003; GRIGIO *et al.*, 2004), where NV exposes the weaknesses of the environment, including physical factors such as geology, geomorphology, slope, pedology and vegetation. EV assesses the environment's susceptibility to potential impacts caused by anthropic use. The term vulnerability of the natural physical environment, or physical vulnerability (BUSMAN *et al.*, 2016), distinguishes between the higher or lower stability of the physical variables of ecosystems, according to Tricart's principle of ecodynamics (1977). According to this concept, physical variables are considered more stable and thus less vulnerable when pedogenetic processes predominate, and less stable and therefore more vulnerable, when morphogenetic processes dominate.

To estimate the physical vulnerabilities of seashores to climate change, a weighted version was designated Coastal Vulnerability Index (CVI), using coastal geomorphology, slope, changes in RSL, significant wave height, mean tidal amplitude and historical changes in the CL (GORNITZ, 1991; GORNITZ *et al.*, 1994). The CVI was later adapted to different regional and local coastlines around the world (THIELER; HAMMAR-KLOSE, 2000; BORUFF *et al.*, 2005; OZYURT, ERGIN, 2010; MARTINS, 2015; BUSMAN *et al.*, 2016; PANTUSA *et al.*, 2018; GERRITY *et al.*, 2018).

Thus, vulnerability to erosion is a spatial concept used to identify coastal stretches and socioeconomic activities susceptible to disturbances resulting from coastal erosion (BEVACQUA *et al.*, 2018). In this respect, maps of coastal vulnerability to erosion contribute to planning sustainable land use and cover, understanding the impacts of coastal dynamics and seashore resilience, but with different execution scales (regional to local), combining usable resources in the formulation of public policies for integrated coastal management (ZHU *et al.*, 2019). On the local scale, these studies are particularly relevant in assessing the factors that will affect the current state of the seashore in the face of possible disasters, helping reduce coastal risks caused by extreme climatic events and increased RSL (PARTHASARATHY *et al.*, 2015).

The aim of this article was to define and assess physical vulnerability indices on the coast of Barreira do Inferno, in the municipality of Parnamirim, Rio Grande do Norte state (RN), Brazil, an area of permanent environmental preservation that has been subjected to intense real estate development.

2. STUDY AREA CHARACTERIZATION

The study area covers 24 km², primarily in the Barreira do Inferno Launch Center (CLBI) and part of the surrounding area, with around 11 km of CL, located on the coast of Parnamirim, RN, a metropolitan region south of Natal, the state capital (Figure 1).

This eastern coastline of RN exhibits a tropical dry summer climate (As in Köppen's classification), with widely varying seasonal rainfall, concentrated between April and July, and annual rainfall and temperature of 1,620 mm and 26.3°C, respectively (ALVARES *et al.*, 2013; CARVALHO *et al.*, 2020). Southeast trade winds are dominant, at an estimated 95% occurrence, intensities below 5.2 m/s and 90% with speeds less than or equal to 5.0 m/s, stronger in August and September and weakest in April (BARROS *et al.*, 2013). The regime is semidiurnal mesotidal, with average amplitudes of 2.2 m and 1.1 m for spring and neap tides, respectively (nautical chart DHN/MB, no. 810). East-southeast waves predominate year-round, especially in the summer, from the east, with heights varying significantly from 0.5 to 2.8m (ALMEIDA *et al.*, 2015). The longshore currents carry sediments from south to north (MATOS *et al.*, 2020).

The geological context corresponds to the Natal Shelf and its contiguous continental shelf, located between Alto de Mamanguape to the south and Alto de Touros to the north, which has stratigraphic correlations with the Potiguar Basin and contact with the Paraíba-Pernambuco Basin in the Mamanguape fault (BARBOSA *et al.*, 2007). The Natal Shelf is arranged in grabens and horsts in the NE (40°-60°Az) and NW (300°-320°Az) directions that govern the geological units of the crystalline basement, the lithological units of the Cretaceous, and lithofacies of the Barrier Formation of the Miocene–Pliocene (BEZERRA *et al.*, 2001). The active sea cliffs present at the eastern edge of the CLBI feature outcrops of sedimentary lithofacies of the Barreira Formation, where intercalations and interfingerings of conglomerates, sandstones and mudstones denote continental depositional systems of intertwined and meandering alluvial and fluvial fans (ARAÚJO *et al.*, 2006). This alignment of active sea cliffs forms the border of the Coastal Tableland in the study area, with a slope of up to 20m and flat top overlain by Quaternary units including alluvial terraces, such as on the banks of the Pium River along the southeastern and southern border of the study area, as well as eolian sediments in the mobile dunes and those fixed by vegetation.

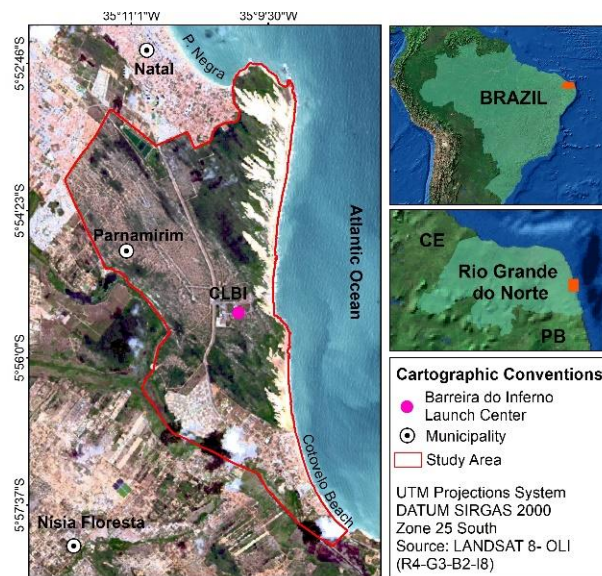


Figure 1 – Study area at the edge of the Barreira do Inferno Launch Center (CLBI) and part of the surrounding area, municipality of Parnamirim, east coast of Rio Grande do Norte state.

The dominant soils are Quartzarenic Neosols, whose origin is related to post-beach eutrophic marine sands and dune fields, and Red-Yellow Argisols originating from weathering of the sedimentary lithofacies of the Barreiras Formation (SANTOS *et al.*, 2018; CPRM, 2010).

The dominant vegetation is Semideciduous Seasonal Forest and Restinga Forest, both belonging to the Atlantic Forest domain (VELOSO *et al.*, 1991), with elements of Caatinga and Coastal Tableland (FRACASSO, 2005).

The CLBI is a permanent preservation area (PPA) used as a military base, with a preponderance of mobile and fixed dune fields, the latter covered with vegetation that is preserved as much as possible. However, portions of the surrounding area have suffered increasing pressure from human occupation, especially in the southern part bordering Cotovelo beach and the northern section adjacent to Ponta Negra Beach, both undergoing intense real estate development.

3. METHODOLOGY

In the analysis of NV, EV and CVI, some of the methodological procedures proposed by Grigio *et al.* (2004), Busman (2016) and Busman *et al.* (2016) were adopted, based on the spatial and statistical analysis of thematic maps of the physical environment, land use and cover. These thematic maps used a 1:50,000 scale after interpretation of multispectral and multitemporal LANDSAT satellite images, submitted to digital imaging processing (DIP) in a geographic information system (GIS).

3.1. Creating Thematic Maps

The creation of thematic maps (Figure 2) relied on previous map surveys with scales of 1:100,000 and 1:250,000, selected from digital data repositories of public institutions: geology, with a scale of 1:100,000 (Brazilian Geographic Service/Mineral Resources Research Company - SGB/CPRM), geomorphology, vegetation and soils, both with a scale of 1:250,000 (Brazilian Institute of Geography and Statistics – IBGE and the Brazilian Agricultural Research Company – EMBRAPA), slope, with a scale of 1:25,000 (State Department of Tourism of RN - SETUR and State Department of Infrastructure - SIN), as shown in Table 1. After the natural and anthropic variables were determined, all the maps were created with a scale of 1:50,000 and the same cartographic basis, with SIRGAS 2000 Datum and the Universal Transverse Mercator (UTM) coordinate system (Zone 25-South), in a GIS environment. The 1:50,000 scale is in line with Ministry of Environment guidelines for creating instruments to guide planning in areas of high-risk and environmental sensitivity, to correlate with the broader regional context (MMA, 2004).

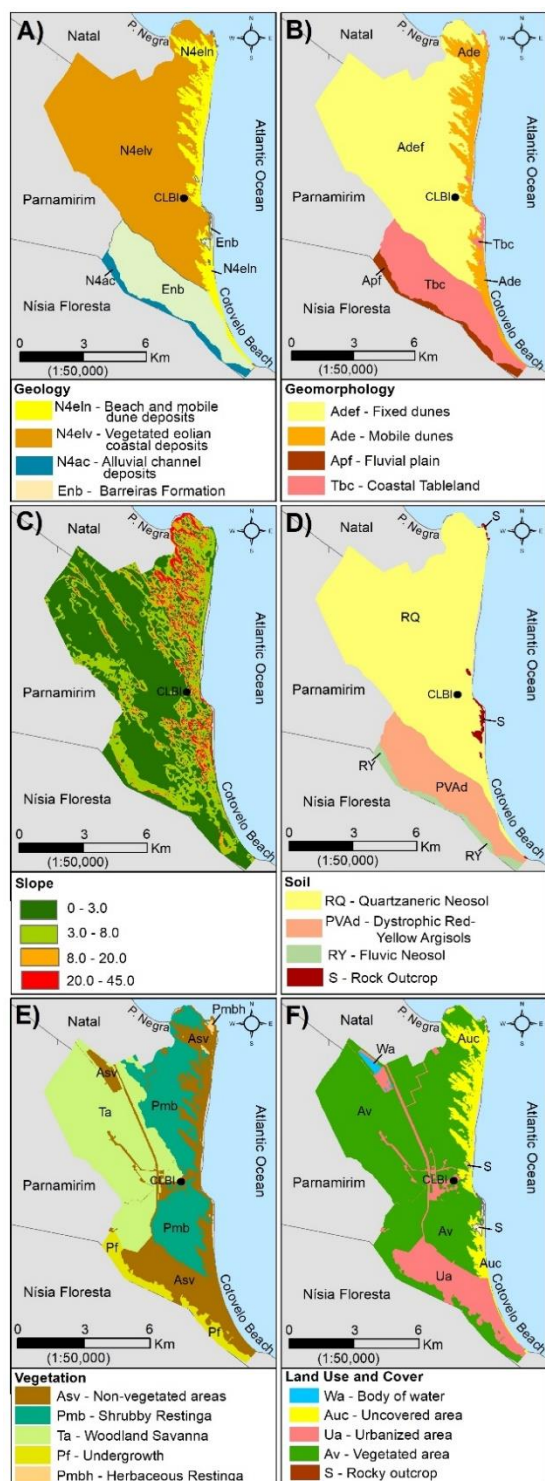


Figure 2 – Thematic maps of the study area in the CLBI: (A) Geology; (B) Geomorphology; (C) Slope; (D) Pedology; (E) Vegetation; (F) Land use and cover.

Table 1 – Digital database sources of public repositories to create updated thematic maps of the study area.

Thematic Maps	
Slope Map	Source: Vector data of the Dune Coast Project, with aerophotogrammetric restitution, of the State Department of Tourism (SETUR) and State Department of Infrastructure (SIN), reprocessed in GIS environment.
Geologic Map	Source: Vector data of the Geological Survey of Brazil-Mineral Resources Research Company (SGB-CPRM), Natal Page SB.25-V-C-C, reprocessed in GIS environment.
Geomorphological Map	Source: Vector data of the Brazilian Institute of Geography and Statistics (IBGE), Page SB-25, reprocessed in GIS environment.
Soil Map	Source: Vector data of the Brazilian Institute of Geography and Statistics (IBGE), Page SB-25, reprocessed in GIS environment.
Vegetation Map	Source: Vector data of the Brazilian Institute of Geography and Statistics (IBGE), Page SB-25, reprocessed in GIS environment.
Land Use and Cover Map	Source: Digital image submitted to supervised classification.

3.2. Coastline (CL) detection

In the prior map survey, the multispectral LANDSAT 5-TM and LANDSAT 8-OLI images of 1984, 1993, 2005 and 2015 were selected from the online catalogs of the National Space Research Institute (INPE) and United States Geological Survey (USGS) to diagnose the dynamic evolution of the CL extension, erosion and accretion rates, based on the statistical modules of the Digital Shoreline Analysis System (DSAS, USGS). In order to reduce uncertainties in the calculation of erosion and accretion rates, as a representative result of the long-term sedimentary dynamic (1984 to 2015), the images analyzed showed similar high tides (1.22 to 1.76m) at the time of imaging.

The images were submitted to radiometric calibration, atmospheric and technical correction of edge enhancement using the Normalized Difference Water Index (NDWI); GAO, 1996), thereby increasing vectorization accuracy. The Digital Elevation Model (DEM) was obtained from the altimetric data of the Shuttle Radar Topography Mission (SRTM) with spatial resolution of 30m, from USGS online data. The multispectral images used were the visible-infrared (bands 1 to 5 and 7 of LANDSAT 5-TM, and bands 1 to 7 of LANDSAT 8-OLI), with spatial resolution of 30m, and panchromatic ranges (band 8 of LANDSAT 8-OLI), with spatial resolution of 15m.

Image georeferencing was conducted in the Universal Transverse Mercator (UTM) map projection, Zone 25-South, SIRGAS 2000 Datum, the ellipsoid of Geodetic Reference System 1980. Distortions and degradations in the LANDSAT 5-TM images of 1984, 1993 and 2005 were corrected, with a mean squared error of less than 0.5 and verifying the geometric corrections made to the LANDSAT 8-OLI images of 2015. Finally, statistical analysis of the multispectral bands was conducted to determine correlations, which favored the selection of DIP techniques.

Table 2 presents the DIP treatments to enhance thematic features, such as the RGB (Red-Green-Blue) color system using isolated bands and band ratios. The panchromatic LANDSAT 8-OLI image (band 8) was integrated to the Intensity (I) layer of the hybrid RGBI (Red-Green-Blue-Intensity) color system, determining the spatial resolution for 15m and underscoring the textural properties of surface features. The set of multispectral images was assessed for spectral redundancy in multivariate analysis using Principal Component Analysis (PCA). The principal components with the lowest correlation were selected as isolated bands in the RGB and RGBI systems. All the triplets selected for the best visual quality underwent histogram contrast adjustment.

The best multispectral band triplets of LANDSAT 8-OLI in 2015 were interpreted and vectorized in a GIS environment to create the following maps: geology (Figure 2A); geomorphology (Figure 2B); slope, derived from the DEM (Figure 2C); soils (Figure 2D), vegetation (Figure 2E), land use and cover (Figure 2F). These thematic maps were readapted from pre-existing maps, with different scales, and thematic classes were considered based on hybrid RGBI images and confirmed in field surveys compatible with the 1:50,000 scale.

Table 2 – Color compositions in the RGB and RGBI color systems and DIP techniques.

Color Systems de Cores	Color Compositions Coloridas	Band Ratios	PC
RGB	R(5)/G(4)/B(3)	R(6/4)/G(5/7)/B(7)	R(PC1)/(PC3) B(PC6)
	R(6)/G(5)/B(2)	R(5) G(3) B(NDWI)	R(PC5)/G(PC4)/B(PC6)
	R(7)/G(6)/B(4)	R(7/5)/G(6/4)/B(5/3)	
RGBI	R(5)/G(4)/B(3)/I(8)	R(5/4)/G(6)/B(5/3)/I(8)	R(PC5)/G(PC6)/B(PC7) I(8)
	R(6)/G(5)/B(2)/I(8)		

Legend: RGB = Red-Green-Blue primary color system; RGBI = Red-Green-Blue-Intensity hybrid color system; NDWI = Normalized Difference Water Index = $(\text{Band}_{\text{Green}} - \text{Band}_{\text{Near Infrared}}) / (\text{Band}_{\text{Green}} + \text{Band}_{\text{Near Infrared}})$; PC = Principal Components.

3.3. Creation of Natural Vulnerability and Environmental Maps

The variables of the physical environment were assessed according to the Analytic Hierarchy Process (AHP) proposed by Saaty (2008) to derive priority weights, by conducting pairwise comparisons of criteria with respect to their importance, using a square matrix, following the values attributed by decision makers in a continuous 9-point weighted scale that varies between extremely to equally, for more or less important contribution of the variable towards the established goal (Table 3).

Table 3 – 9-point scale of relative importance values used for paired comparison between variables. EXT= Extremely; VS = Very Strongly; S = Strongly; M = Moderately; EQUAL = Equally.

EXT	MS	S	M	EQUAL	M	S	MF	EXT
1/9	1/7	1/5	1/3	1	3	5	7	9
← LESS				MORE →				

In the square matrix, each box is filled with a value according to this continuous scale of relative importance between pairs (Table 4). Since there are multiple ways to assess the relative importance of the variables in the paired comparison matrix, Saaty (2008) suggested determining a mathematical indicator of the consistency of comparisons attributed to the pairs, as a function of the size of the matrix and the maximum eigenvalue, denominated the consistency rate (CR). The CR indicates the likelihood of matrix values having been generated by chance, which Saaty (1991) suggests is acceptable when the consistency of preferences is kept below 0.1 (or 10%); it was 0.09 for the study area.

Table 4 – Paired comparison and consistency rate applied to establishing weights in the Natural Vulnerability (NV) index for physical environment variables.

Weight	VAR	GEOM	SLO	SOIL	VEG	GEO
0.25	GEOM	1	1/3	3	3	3
0.42	SLO	3	1	3	3	5
0.10	SOIL	1/3	1/3	1	1/3	3
0.16	VEG	1/3	1/3	3	1	3
0.07	GEO	1/3	1/5	1/3	1/3	1

Consistency Rate: 0.09 (acceptable)

The AHP results were used as the weight in the map algebra (Table 5) and calculation involved the linear combination of each variable multiplied by the resulting weight of AHP to create the NV map (Equation 1). The weights obtained for EV (Equation 2) resulted from the inclusion of land use and cover, deriving the low anthropization influence in the study area.

$$NV = 0.25 \times GEOM + 0.07 \times GEO + 0.16 \times VEG + 0.10 \times SOIL + 0.42 \times SLO \quad (1)$$

$$EV = 0.21 \times GEOM + 0.06 \times GEO + 0.17 \times VEG + 0.09 \times SOIL + 0.36 \times SLO + 0.11 \times USE \quad (2)$$

Where: NV = Natural Vulnerability; EV = Environmental Variability; GEOM = Geomorphology; GEO = Geology; VEG = Vegetation; SOIL = Soils; SLO = Slope; USE = Land use and cover.

Table 5 – Summary of weights resulting from Analytical Hierarchy Processing used in the map algebra to calculate the Natural and Environmental Vulnerability.

Thematic Variables	Natural Vulnerability	Environmental Vulnerability
Slope	0.42	0.36
Geomorphology	0.25	0.21
Vegetation	0.16	0.17
Soils	0.10	0.09
Geology	0.07	0.06
Land use and cover	-	0.11
TOTAL	1.0	1.0

The NV and EV indices proposed by Grigio *et al.* (2004) are based on the degree of vulnerability to erosion stipulated for each thematic class, varying in intervals of 0.5 between scores of 1 (stable), 2 (intermediate) and 3 (unstable), according to the concept of physical characteristic stability, where the pedogenetic and morphogenetic processes, respectively, predominated (TRICART, 1977; CREPANI *et al.*, 2001). In this respect, after statistical analyses in Boolean logic, the thematic variable classes of the physical environment were converted into five classes, which range from very low to very high (BUSMAN, 2016; BUSMAN *et al.* 2016), according to the scores in Table 6.

Table 6 – Vulnerability class ranges and scores according to Boolean logic.

Very Low	Low	Average	High	Very High
1.0 – 1.4	1.4 – 1.8	1.8 – 2.2	2.2 – 2.6	2.6 – 3.0

The scores used for each of the thematic classes are summarized in Table 7.

Likewise, the thematic variables used in EV and NV were compared by PCA, according to the proportion of physical vulnerability classes of Table 7. Principal components (PCs) are used to assess the redundancy connections between the thematic classes and identify those with the greatest influence in each PC, when the eigenvalue is higher than [0.7]. According to Lattin *et al.* (2011), values above [0.5] indicate a moderate to strong linear correlation.

3.4. Coastline Evolution to Determine the Coastal Vulnerability Index

Erosion and deposition rates that occur along the CL were assessed using the Coastal Vulnerability Index (CVI). In this method, it is suggested that the multisource physical and dynamic variables that influence coastal resistance to erosion be parametrized, as proposed by Gornitz *et al.* (1994) and adapted by Özyurt and Ergin (2009) and Martins (2015). The following physical environment variables were considered: geomorphology (Figure 2B), slope (Figure 2C), type of infrastructure or activity

installed on the CL, variation rate and CL prognoses. The dynamic variables were variation in tidal amplitude, significant wave height, and scenarios of increased RSL. These factors contribute to the risk of erosion and, consequently, flooding on specific stretches of the CL, considering the adaptation of CVI to the characteristics of the study area (ÖZYURT; ERGIN, 2009, 2010; FERNÁNDEZ *et al.*, 2013; BUSMAN, 2016).

Table 7 – Thematic class scores for vulnerability indices using Boolean logic.

Slope		Geology	
Classes	Scores	Classes	Scores
0° – 3°	1.0	Non-vegetated coastal eolian deposits	3.0
3° – 8°	2.0	Vegetated coastal eolian deposits	2.5
8° – 20°	2.5	Alluvial deposits	2.0
20° – 65°	3.0	Barreiras Formation	1.5
Geomorphology		Soils	
Classes	Scores	Classes	Scores
Mobile Dunes	3.0	Quartzarenic Neosols	3.0
Fixed Dunes	2.5	Fluvic Neosols	2.5
Fluvial plain	2.0	Red-Yellow Argisols	2.0
Coastal tableland	1.0	Rocky outcrop	1.0
Vegetation		Land use and Cover	
Classes	Scores	Classes	Scores
Herbaceous Restinga	3.0	Open areas	3.0
Bushy Restinga	2.5	Vegetated area	2.5
Woodland savanna	2.0	Urbanized area	2.0
Ground vegetation	2.0	Rocky outcrop	1.0
Vegetation-free area	1.0	Water body	0

Equation 3 was used to calculate the CVI, based on the simple arithmetic mean without weighting in order to maintain the physical and hydrodynamic variables equally relevant, according to the methodology proposed by Busman (2016). In this method, the segments of the CL are classified into five CVI classes, varying between 1 for the least to 5 for the most vulnerable.

$$CVI = \frac{(GEOM + CLV + SLO + ALT + AMP) + SCE + PROGCLV + INFRA + USE}{9} \quad (3)$$

Where: CVI = Coastal Vulnerability Index; GEOM = Geomorphology; CLV = Coastline variation; SLO = Slope; ALT = Significant wave height; AMP = tidal amplitude; SCE = Scenarios for the increase in relative sea level (RSL); PROGCLV = Prognosis of coastline variation; INFRA = Infrastructure installed on the CL; USE = Type of use or activity.

The rate of RSL increase accompanies the proposals of future Representative Concentration Pathway (RCP) scenarios proposed by the Intergovernmental Panel on Climate Change (IPCC.), as presented in the Fifth Assessment Report (IPCC, 2014), between the most optimistic projections (RCP 2.6) of an average rate of RSL increase of 4.4 mm/year; rate of increase of about 6.1 mm/year in the intermediate scenario (RCP 4.5); and 11.2 mm/year in the most pessimistic scenario (RCP 8.5).

The tidal amplitude data were obtained from the tide tables of the Hydrography and Navigation Directorate database (DHN, Brazilian Navy) for the port of Natal from 1973 to 2012. The significant wave height data on the CL were extracted from the Coastal Modeling System of Brazil (SMC Brazil) for Barreira do Inferno coastal zone (MATOS *et al.*, 2020).

The variations in the CL, obtained from multispectral and multitemporal images by calculating the erosion and accretion rates in Digital Shoreline Analysis System software v.4.0 (DSAS) in a GIS environment (THIELER *et al.*, 2009), were based on transects spaced 50 m apart. Statistical analyses involved the use of Net Shoreline Movement (NSM) modules that assess the distance between the oldest CL and a more recent one over a certain analysis period, and least square regression of the Linear Regression Rate (LRR) was applied to calculate erosion and accretion rates.

4. RESULTS AND DISCUSSION

The variables classified to analyze NV and EV indices were physical environment, geomorphology, slope, vegetation, geology, soils, land use and cover, obtained in DIP treatments applied on multispectral LANDSAT 5-TM and LANDSAT 8-OLI images and confirmed in field surveys at a scale of 1:50,000.

The thematic classes of slope, geomorphology and vegetation are the most relevant for defining NV and EV behavior, with a significant value of 83 and 74% of the total weights in these indices, respectively (Table 5). Soil classes influenced NV by 10%, and type of land use and cover EV by 11%, considering the designated use for military activities, with relatively little anthropogenic change in the natural characteristics of the study area. The physical variables inherent to geomorphology, slope, vegetation and soils were greater influencers of susceptibility to erosion, flooding and mass movements in coastal zones. Since they are conditioned to changes in the geological time scale, the geology classes receive the lowest weights. With the presence of vegetation, there is less soil susceptibility to erosion, while land use and cover reflect the rapid changes that occurred in the physical context of a given region. These facts justify the use of weights obtained in AHP, which, despite being based on values attributed by scientists and public administrators, generally reduce subjectivity and redundancy in determinations of the importance of variables when incorporating the hierarchical consistency between them in weighting. Likewise, and with a view to reducing the size of thematic variables, the PCs that represent 95 and 99% of the accumulated variance in EV and NV indices, respectively, were determined, accounting for the original information in PC1, PC2, PC3 and PC4. The recurring variable with the highest weight was vegetation in PC1 in EV and NV, geomorphology and geology in PC2 in EV and NV, slope in PC3 in NV and land use and cover in EV, and soils in PC4 in NV.

The sectors with VI in the average, high and very high classes on the NV map correspond to 75% or 18 km² of the total area (Figure 3A, Table 8). The map of the resulting NV (Figure 4) underscores the relevance of the physical environment classes in the control of NV in sectors of the coastal zone. The areas of average, high and very high NV are concentrated in the mobile dunes and those fixed by shrubby vegetation that exhibit classes with slopes of more than 20° and Quartzarenic Neosols, a set of factors that characterize the area as highly susceptible to morphogenetic processes. In the geological aspect, there is obvious correspondence with non-vegetated (mobile dunes) and vegetated coastal eolian deposits and sandy beaches. The low and very low NV classes correspond to 25% of the study area, defining the sectors with a predominance of rocky outcrops in the Barreiras Formation and fluvial plain deposits of the Pium River, in the context of the relatively flat Coastal Tableland (slope < 8°), with Red-Yellow Dystrophic Argisols and covered by ground vegetation or none at all. It is important to underscore that in NV analysis, only the physical variables that interact with all the physical properties in the area are considered. This indicates that the dominant thematic classes in the study area consistently exhibit high and very high natural susceptibility to the physical environment processes, which promote local changes such as sediment detachment, transport and deposition, given the local climate and hydrodynamic conditions. There is evidence of low sediment cohesion and therefore low stability in the thematic class components of the physical environment, especially where the vegetation cover is sparse or absent, in the fissures and ravines in areas of water flow concentrated on the rocky outcrops of the Coastal Tableland, the face of the active sea cliffs at the eastern edge, in addition to sandslides on the faces of dunes at the northeastern border, as occurs on the leeward side of the Morro do Careca (Bald Hill). This is one of the factors responsible for the decline in the volume of sediments at this important tourist attraction (AMARO *et al.*, 2015).

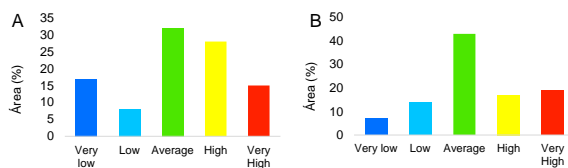


Figure 3 – Percentage distribution of vulnerability classes in relation to the total study area: (A) Natural Vulnerability; (B) Environmental Vulnerability.

Table 8 – Characteristics of the Natural Vulnerability indices and classes in the study area.

Natural Vulnerability Map			
VI	Classes	Area (km ²)	Area (%)
1 – 1.57	Very Low	4.0	16.7
1.57 – 1.99	Low	2.0	8.3
1.99 – 2.41	Average	7.7	32.1
2.41 – 3.00	High	6.7	27.9
3.00 – 3.67	Very High	3.6	15.0
TOTAL		24.0	100

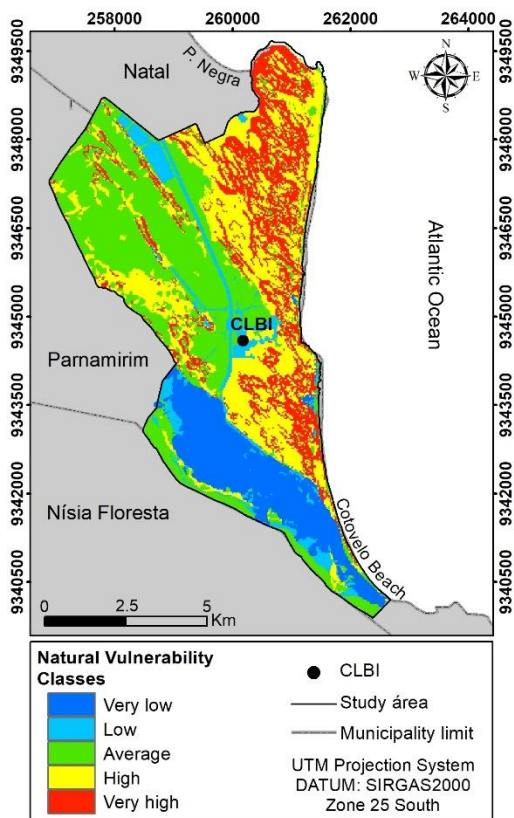


Figure 4 – Natural Vulnerability (NV) map distributed into classes for the Barreira do Inferno Launch Center (CLBI).

In the EV map, the VIs of the average, high and very high vulnerability classes represent 79.1% or 19 km² of the total CLBI area (Figure 3B, Table 9). Figure 5 shows the EV map with an 18.7% increase for the very high class in the sector dominated by mobile dunes and those fixed by shrubby vegetation, with slopes of more than 20° and predominance of Quartzarenic Neosols. Average vulnerability increased to 43.7% or 10.5 km² of the total study area (Figure 3B, Table 9), encompassing most of the dunes fixed by vegetation cover and with flat morphology (slope < 3°), where the main urbanized areas are located. It is noteworthy that the study area still consists of natural environments with little anthropic influence.

There was an increase of high to very high EV classes in the areas at the eastern and northeastern borders of the study area, where the active cliffs of the Barreiras Formation, sandy beaches and fixed and mobile dunes are located, including Morro do Careca. Another marked aspect was the decline in low and very low vulnerability classes to 20.9% or 5 km² of the total study area, restricted to Barreira Formation outcrops on the top of the Coastal Tableland, Dystrophic Red-Yellow Argisols with sparse vegetation, and urbanized sectors with some infrastructure, such as those containing the CLBI facilities. Anthropoc occupation of the CLBI occurred exclusively in the flat portion of the fixed dune field and the Coastal Tableland, initially with the removal of vegetation only in the specific areas of the facilities and road

accesses, such as highway RN-063. However, anthropic occupation near the coastline, along with the active cliffs and sandy beaches, such as the urbanized area of Cotovelo Beach, are surrounded by high and very high NV and EV classes. It is important to underscore the environmental complexity of the geographic position of the urbanized stretch of Cotovelo beach between the coastline and the fluvial plain of the Pium River. The Pium River, along with other tributaries (Pitumbu, Taborda and Água Vermelha), is part of the Pirangi watershed, essential to the population of the municipality of Parnamirim, especially in the coastal sector, which uses its waters for agriculture, drinking and bathing. These facts demonstrate the infeasibility of uncontrolled urban expansion in these sectors, without new urban projects causing environmental damage and exposing old and new settlements or infrastructures to the risks inherent to coastal processes, particularly the increase in hydrodynamic forcing (waves, tides, currents and winds) in the continuous scenarios of climate change (AMARO *et al.*, 2015; MATOS *et al.*, 2020).

Table 9 – Characteristics of Environmental Vulnerability indices and classes at the Barreira do Inferno Launch Center (CLBI).

Environmental Vulnerability Map			
VI	Classes	Area (km ²)	Area (%)
1 – 1.35	Very Low	1.6	6.7
1.35 – 2.05	Low	3.4	14.2
2.05 – 2.56	Average	10.5	43.7
2.56 – 3.00	High	4.0	16.7
3.00 – 3.62	Very High	4.5	18.7
TOTAL		24.0	100

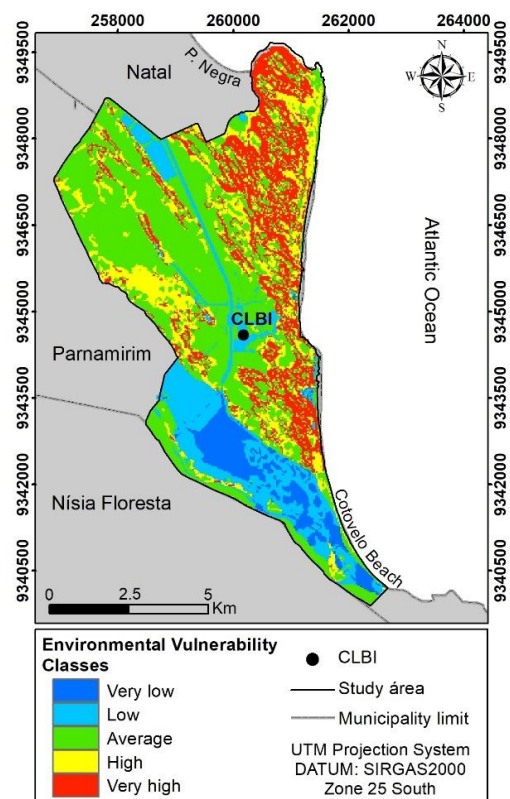


Figure 5 – Environmental Vulnerability (EV) Map distributed in classes for the Barreira do Inferno Launch Center (CLBI).

Using this bias driver, evolutionary analysis of the CLs over a 31-year period with DSAS in a GIS environment to calculate the CVI, was based on LANDSAT images in 1984, 1993, 2005 and 2015. The CL assessed contains stretches with deposits of up to 40.75 m and others with beach erosion reaching -53.74 m wide between 1984 and 2015, as shown in the central tendency measures of this distribution (Table 10). For the entire CL of the CLBI, the average erosion rate was -0.21 m/year, corresponding to a retreat of -10.23 m of the CL during the time period analyzed, the highest rates being -1.69 m/year of erosion and 1.32 m/year of accretion. Thus, there was greater retreat than accretion in the CL stretches between 1984 and 2015; however, these gains and losses still occur in equal proportions, likely because it is a coastline with an extensive preserved stretch and low anthropic occupation in the CLBI. These CL variations are compatible with the trend towards sedimentary dynamics on the eastern coast of RN, with waves coming predominantly from the E and SE, following the seasonal changes of the trade winds, which promotes longitudinal sediment transport of around 50,000 m³/year from the south to the north (MATOS *et al.*, 2019). One restriction to consider is that, even with the best approximations using similar tidal conditions as those on the date of LANDSAT imaging, there is a difference of 50 cm between the tidal level of the 1984 image in relation to the other images, which may overestimate the limits of the CL and indicate greater erosion in the period, given the geomorphological context of the sandy beach with a low slope.

Table 10 – Statistical description of the CL variation.

DESCRIPTIVE STATISTICS	RSL (m)	LRR (m/year)
Average	-10.23	-0.21
Standard deviation	18.84	0.63
Variance	354.86	0.40
Maximum Erosion	-53.74	-1.69
Maximum Accretion	40.75	1.32

Figure 6 shows the CVI obtained for the projected scenarios of the representative concentration pathway (RCP) of the Intergovernmental Panel on Climate Change (IPCC) (2014), considering the average variation in RSL, with high confidence until 2100, as follows: average of 0.44 mm (0.28 to 0.61 mm) in RCP 2.6; 0.53 mm (0.36 to 0.71 mm) in RCP 4.5; and 0.74 mm (0.52 to 0.98 mm) in RCP 8.5.

For RCP 2.6 and RCP 4.5, the entire coastline exhibited low vulnerability. RCP 8.5 displayed stretches of moderate vulnerability, representing 31% of the CL, predominantly in active sea cliffs and sandy beaches, sectors still free of anthropic activity since they are located inside the CLBI.

The construction of the CVIs based on RCP projections used highly reliable global data as guiding parameters, in order to assess CLs still in their natural state, with no infrastructure. However, recent data based on a marigraph and satellite altimeter time series suggested that the average increase in RSL in the world was 3.3 mm/year between 1995 and 2015 (HANSEN *et al.*, 2016). This is compatible with the rise in RSL on the Brazilian equatorial coast, based on reviews of marigraph and satellite altimeter time series (since 1946), revealing an increase between 2.0 and 5.6 mm/year for the sector between Salvador, Bahia state and Recife, Pernambuco state (HARARI; CAMARGO, 1994; MUEHE, 2006; LOSADA *et al.* 2013; KLEIN; SHORT, 2016).

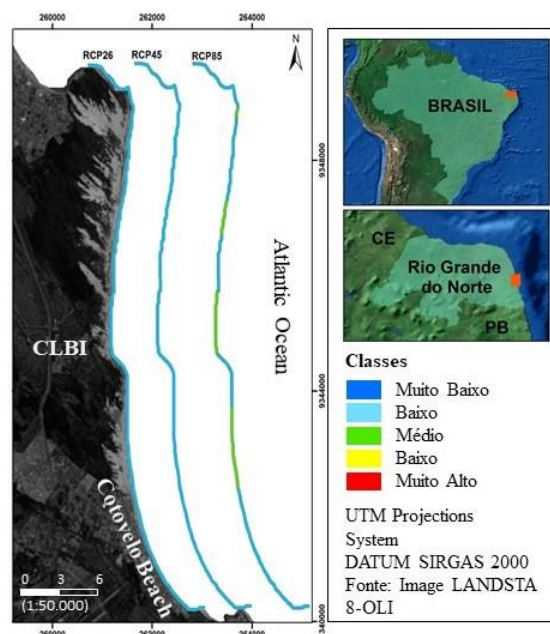


Figure 6 - Coastal Vulnerability Index for RCP 2.6, RCP 4.5 and RCP 8.5 scenarios of the IPCC (2014) on the coastline of the Barreira do Inferno Launch Center (CLBI).

5. FINAL CONSIDERATIONS

This article assessed the dominant thematic classes of the physical environment, slope, geomorphology, vegetation, soils, geology, land use and cover, and categorized the most influential in creating EV, NV and CVI maps for the CLBI coastline on a 1:50,000 scale. Analyses and interpretations of variables and thematic classes and CL variation were based on color compositions in the RGB and RGBI systems of multispectral and multidimensional LANDSAT images from 1984, 1993, 2005 and 2015, integrated into a GIS environment and confirmed in field surveys.

Using multicriteria AHP methods attenuated the subjectivity of interpretations of the thematic variables of the physical environment, confirmed by the decline in redundancy, according to principal component analysis and combined with analysis of thematic classes using Boolean operators, where slope, geomorphology and vegetation are the most relevant in determining performance. The variables and thematic classes were weighted in the calculations of NV, EV and CVI.

The VI of average, high and very high classes predominate on the NV map, covering 75% or 18 km² of the total area, demonstrating the importance of mobile and fixed dunes where slopes of more than 20° and Quartzarenic Neosols dominate. On the EV map, average, high and very high vulnerability classes are observed in 79.1% or 19 km² of the total area, particularly the latter in the mobile and fixed dunes.

The variation in CL between 1984 and 2015 showed erosion values of around -53.74 m and deposition of up to 40.75 m (Table 10). The average erosion rate along the entire CL was -0.21 m/year, corresponding to a retreat of -10.23 m, with maximum rates of -1.69 m/year of erosion and 1.32 m/year of accretion in

the period. As such, and considering the synergy between the physical environment variables and the significant maximum wave height and tidal amplitude, the CVI was created for future scenarios of RCP 2.6 (optimistic), RCP 4.5 (moderate) and RCP 8.5 (pessimistic). The entire CL showed low vulnerability in the RCP 2.6 and RCP 4.5 scenarios. In the RCP 8.5 projection, 31% of the CL exhibited moderate vulnerability, especially the active sea cliffs and sandy beaches in the CLBI, with no anthropic occupation.

However, the data for the Atlantic equatorial coastline indicate an increase in the frequency of extreme climate events, hydrodynamic forcing energy and primarily, a rise in RSL (between 2.0 and 5.6 mm/year), demonstrating the current unfavorable climate conditions, whose future scenarios tend to worsen. The CLBI geographic features have an influence on the local and regional ecosystem balance, since it is a permanent preservation area with active sea cliffs and conserved vegetation cover that fixes the dunes, and no anthropic facilities on the CL. It is also important to keep the CL in the study area free of anthropic facilities, since it is responsible for the sedimentary balance of Ponta Negra Beach and Morro do Careca, which is undergoing intensive sedimentary depletion caused by the disordered settlement of the coastline, and climate change. Anthropometric changes on the coast of Barreira do Inferno, disregarding the aspects related to this article, will intensify the erosion process in adjacent coastal sectors and, consequently, the environmental impacts of erosion and flooding in the occupied areas.

Thus, the methodological strategy adopted, based on multispectral and multidimensional hybrid color images, was suitable to create the thematic maps of the physical environment, land use and cover, NV and EV at a 1:50,000 scale, and relevant for public managers to use in territorial planning of the coastline. The decision-making algorithms of GIS, AHP, Boolean logic and PCA proved to be efficient tools in the qualitative and quantitative selection of thematic alternatives in VI analyses. The resulting EV, NV and CVI underscore the significant influence of the physical environment variables of the current coastal region, especially given the future projections of increasing extreme climate events. Thus, the materials and methods used are applicable to other sectors of the equatorial Atlantic coast. The VIs will also be stipulated in the future by changes in governmental decisions and actions regarding the use and occupation of the coastline, given the unavoidable adaptations to and mitigation of the dangers of coastal erosion. It is suggested that the variables and thematic classes of the physical environment and their dynamics be further investigated using other high-performance applied geotechnology techniques, such as high-resolution satellite images or Remotely Piloted Aircraft orthophoto mosaics to assess short-term changes along the coastline (annual and seasonal) and create more detailed maps. Moreover, it is recommended that spatial analysis methods be broadened (fuzzy logic, neural networks, decision tree analysis) when assessing the changes and transitions of thematic classes. Considering the applicability of the results obtained for the VI, it is suggested that erosion risk maps be created to support coastline management.

6. REFERENCES

- ALMEIDA, L. R.; AMARO, V.E.; MARCELINO, A. M. T.; SCUDELARI, A.C. Avaliação do clima de ondas da praia de Ponta Negra (RN, Brasil) através do uso do SMC-Brasil e sua contribuição à gestão costeira. *Revista de Gestão Costeira Integrada*, v.15, n.2, p.135-151, 2015.
- ALVARES, C. A.; STAPE, J. L.; SENTELHAS, P. C.; GONÇALVES, J. L. M.; SPAROVEK, G. Köppen's climate classification map for Brazil. *Meteorologische Zeitschrift*, Stuttgart, v. 22, n. 6, p. 711-728, 2013.
- AMARO, V. E.; GOMES, L. R. S. ; LIMA, F. G. F.; SCUDELARI, A. C.; NEVES, C. F.; BUSMAN, D. V.; SANTOS, A. L. S. Multitemporal Analysis of Coastal Erosion Based on Multisource Satellite Images, Ponta Negra Beach, Natal City, Northeastern Brazil. *Marine Geodesy*, Oxfordshire, v. 38, p. 1-25, 2015.
- ARAÚJO, V.; REYES, Y.; LIMA, R.O.L.; PELOSI, A.P.M.R.; MENESES, L.; CÓRDOBA, V.C.; LIMA-FILHO, F.P. Fácies e Sistema Depositional da Formação Barreiras na Região da Barreira do Inferno, Litoral Oriental do Rio Grande do Norte. *Geologia USP Série Científica*, São Paulo, v. 6, n. 2, p. 43-49, 2006.
- BARBOSA, J. A.; NEUMANN, V. H.; LIMA FILHO, M.; SOUZA, E. M.; MORAES, M. A. Estratigrafia da faixa costeira Recife-Natal (Bacia da Paraíba e Plataforma de Natal), NE Brasil. *Estudos Geológicos*, Recife, v.17, n. 2, p.3-30, 2007.
- BARROS, J. D. Sazonalidade do vento na cidade de natal/RN pela distribuição de Weibull. *Sociedade e Território*, Natal, v. 25, n. 2, p. 78-92, 2013.
- BEVACQUA, A.; YU, D.; ZHANG, Y. Coastal vulnerability: Evolving concepts in understanding vulnerable people and places. *Environmental Science & Policy*, Amsterdã, v.82:19–29, 2018.
- BEZERRA, F. H. R.; AMARO, V. E.; VITA-FINZI, C.; SAAD, A. Pliocene-Quaternary fault control of sedimentation and coastal plain morphology in NE Brazil. *Journal South American Earth Sciences*, Amsterdã, v. 14, p. 61–75, 2001.
- BORUFF, B. J.; EMRICH, C.; CUTTER, S. L. Erosion Hazard Vulnerability of US Coastal Counties. *Journal of Coastal Research*, Florida, v. 25, n. 5, p.932-942, 2005.
- BRAGA, R. C.; PIMENTEL, M. A. S. Índice de Vulnerabilidade Diante da Variação do Nível do Mar na Amazônia: Estudo de Caso no Município de Salinópolis-Pará. *Revista Brasileira de Geografia Física*, Recife, v. 12, n. 2, p. 534-561, 2019.
- BUSMAN, D. V. *Zoneamento da dinâmica costeira – aplicação de geotecnologias em apoio à gestão costeira integrada na Praia Atalaia-PA e trecho de praias entre os Municípios de Guimarães e Macau-RN, setor sob influência da indústria*

- petrolífera*. Tese de doutorado apresentado ao Programa de Pós Graduação em Geodinâmica e Geofísica da Universidade Federal do Rio Grande do Norte, 2016, 185p.
- BUSMAN, D. V.; AMARO, V. E.; SOUZA FILHO, P. W. Análise estatística multivariada de métodos de Vulnerabilidade Física em zonas costeiras tropicais. *Revista Brasileira de Geomorfologia*, Rio de Janeiro, v. 17, n. 3, p. 499-516, 2016.
- CARVALHO, A. A.; MONTENEGRO, A. A.; SILVA, H.P. da; LOPES, I.; MORAIS, J.E.F.de; SILVA, T.G.F.da. Trends of rainfall and temperature in Northeast Brazil. *Revista Brasileira de Engenharia Agrícola e Ambiental*, Campina Grande, v. 24, n. 1, p.15-23, 2020.
- CREPANI, E.; MEDEIROS, J. S.; HERNANDEZ, P.; FLORENZANO, T. G.; DUARTE, V.; BARBOSA, C. C. F. *Sensoriamento Remoto e Geoprocessamento Aplicado ao Zoneamento Ecológico-Econômico e ao Ordenamento Territorial*. São José dos Campos: SAE/INPE, 2001.
- FERNÁNDEZ, V., GÓMEZ, M. E GUIGOU, B. Coastal vulnerability index to global change in Uruguay. In: 11TH INTERNATIONAL SYMPOSIUM FOR GIS AND COMPUTER CARTOGRAPHY FOR COASTAL ZONES MANAGEMENT, 2013, Victoria, *Abstract...* Victoria: EUC, 2013.
- FRACASSO, P. *Sistema de dunas do Parque das Dunas e Barreira do Inferno, Natal (RN): levantamento geológico/geofísico, elaboração do modelo determinístico e avaliação da vulnerabilidade/susceptibilidade frente as pressões antrópicas*. Dissertação de mestrado apresentado ao Programa de Pós Graduação em Geodinâmica e Geofísica da Universidade Federal do Rio Grande do Norte, 2005, 184 p.
- GAO, B. NDWI - A normalized difference water index for remote sensing of vegetation liquid water from space. *Remote Sensing of Environment*, Amsterdam, v. 58, n. 3, p. 257-266, 1996.
- GERRITY, B.; PHILLIPS, M. R.; CHAMBERS, C. Applying a Coastal Vulnerability Index to San Mateo County: Implications for Shoreline Management. *Journal of Coastal Research*, Florida, v. 85, p. 1406-1410, 2018.
- GORNITZ, V. M.; DANIELS, R. C.; WHITE, T. W.; BIRDWELL, K. R. The development of a coastal risk assessment database: Vulnerability to sea-level rise in the U.S. southeast. *Journal of Coastal Research*, Florida, v. 12, p. 327-338, 1994.
- GORNITZ, V.M. Vulnerability of the East coast, USA to future sea level rise. *Journal of Coastal Research*, Florida, v.9, p.201-237, 1991.
- GRIGIO, A.M.; SOUTO, M.V.S.; CASTRO, A.F.; AMARO, V.E.; VITAL, H. & DIODATO, M.A. Use of remote sensing and geographical information system in the determination of the natural and environmental vulnerability of the Municipal District of Guamaré, Rio Grande do Norte, Northeast of Brazil. *Journal of Coastal Research*, Florida, v. 39, p.1427-1431, 2004.
- HANSEN, J.; SATO, M.; HEARTY, P.; *et al.* 2016: Ice melt, sea level rise and superstorms: Evidence from paleoclimate data, climate modeling, and modern observations that 2°C global warming could be dangerous. *Atmospheric Chemistry Physics*, Germany, v. 16, p. 3761-3812, 2016.
- HARARI, J.; CAMARGO, R. Tides and mean sea level in Recife (PE): 8° 3.3'S 34° 51.9'W: 1946 to 1988. *Boletim do Instituto Oceanográfico*, 1994.
- IPCC. Fifth Assessment Report. Cambridge: Cambridge University Press, 2014.
- KLEIN, A.H.F.; SHORT, A.D. *Brazilian beach systems*. In Short A.D.; Klein A.H.F. ed. *Brazilian beach systems*. Coastal Research Library. Springer, 2016, p. 1-35.
- KOLLURA, R.V. *Health risk assessment. Principles and practices*. In: *Risk Assessment and Management Handbook*. Kollura, R.V., Bartell, S.M., Pitblado, R.M., Scott-Stricoff, R. eds. McGraw-Hill, 1996.
- KULP, S.A.; STRAUSS, B.H. New elevation data triple estimates of global vulnerability to sea-level rise and coastal flooding. *Nature Communications*, California, v. 10, p. 4844. 2019.
- LATTIN, J.; CARROLL, J. D.; GREEN, P. E. Análise de dados multivariados. *Cengage Learning*, 455p, 2011.
- LOSADA, I.J.; REGUERO B.G.; MÉNDEZ, F.J.; CASTANEDO, S.; ABASCAL, A.J.; MÍNGUEZ R. Long-term changes in sea-level components in Latin America and the Caribbean. *Global Planet Change*, Amsterdã, v. 104, p. 34-50, 2013.
- MARTINS, K. A. *Vulnerabilidade à erosão costeira e mudanças climáticas através de indicadores em Pernambuco*. Dissertação de mestrado apresentada ao Programa de Pós-graduação em Oceanografia da Universidade Federal de Pernambuco, 2015. 107p.
- MATOS, M.F.A.; AMARO, V.E.; SCUDELARI, A.C.; BEZERRA, A.C.N. Análises estatísticas de alturas significativas de ondas de série temporal de curto prazo na costa do Rio Grande do Norte. *Pesquisas em Geociências*, Porto Alegre, v. 46, n. 1, p. 1-24, 2019.
- MATOS, M.F.A.; GURGEL, D.F.; SCUDELARI, A.C.; AMARO, V.E. Estimativa da taxa anual e sazonal do transporte longitudinal sedimentar na zona costeira do Litoral Oriental do Rio Grande Do Norte. *Revista Brasileira de Geomorfologia*, Rio de Janeiro, v. 21, n. 1, p.79-99, 2020.
- MCGRANAHAN, G.; BALK, D.; ANDERSON, B. The rising tide: assessing the risks of climate change and human

- settlements in low elevation coastal zones. *Environment and Urbanization*, Londres, v. 19, n. 1, p. 17-37, 2007.
- MCLAUGHLIN, S.; MCKENNA, J.; COOPER, J.A.G. Socioeconomic data in coastal vulnerability indices: Constraints and opportunities. *Journal of Coastal Research*, Florida, v. 36, p. 487-497, 2002.
- MMA. Especificações e normas técnicas para elaboração de cartas de sensibilidade ambiental para derramamentos de óleo. MMA. 108 p. 2004.
- MUEHE, D. Erosion in the Brazilian coastal zone: an overview. *Journal of Coastal Research*, Florida, v. 39, p. 43-48, 2006.
- NICHOLLS, R. J.; WONG, P. P.; BURKETT, V. R.; CODIGNOTTO, J. O.; HAY, J.E.; MCLEAN, R.F.; RAGOONADEN, S.; WOODROFFE, C. D. *Coastal systems and low-lying areas*. In: Climate Change 2007: Impacts, Adaptation and Vulnerability. 1 ed. Cambridge: Cambridge University Press, 315-356, 2007.
- ÖZYURT, G.; ERGIN. A. Application of sea level rise vulnerability assessment model to select coastal areas of Turkey. *Journal of Coastal Research*. Florida, v. 56, p 248-251, 2009.
- ÖZYURT, G.; ERGIN. A. Improving coastal vulnerability assessments to sea-level rise: A new indicator-based methodology for decision makers. *Journal of Coastal Research*, Florida, v. 26, n. 2, p. 265-273, 2010.
- PANTUSA, D.; D’ALESSANDRO, F.; RIEFOLO, L.; PRINCIPATO, F.; TOMASICCHIO, G. R. Application of a coastal vulnerability index. A case study along the Apulian Coastline, Italy. *Water*, v. 10, n. 9, p. 1218, 2018.
- PARTHASARATHY, A.; NATESAN, U. Coastal vulnerability assessment: A case study on erosion and coastal change along Tuticorin, Gulf of Mannar. *Natural Hazards*, Switzerland, v. 75, p. 1713-1729, 2015.
- SAATY, T. L. Decision making with the analytic hierarchy process. *International Journal of Services Sciences*, Switzerland, v. 1. 2008.
- TAGLIANI, C.R.A. 2003. Técnica para avaliação da vulnerabilidade ambiental de ambientes costeiros utilizando um sistema geográfico de informação. In: SIMPÓSIO BRASILEIRO DE SENSORIAMENTO REMOTO, 11, p. 1657-1664. 2003.
- THIELER, E. R.; HIMMELSTOSS, E. A.; ZICHICHI, J. L.; ERGUL. A. The Digital Shoreline Analysis System (DSAS) version 4.0-an ArcGIS extension for calculating shoreline change. *U.S. Geological Survey*, 2009.
- THIELER, E.R., HAMMAR-KLOSE, E.S. National Assessment of Coastal Vulnerability to Future Sea-Level Rise: Preliminary Results for the U.S. Pacific Coast: *U.S. Geological Survey*, Open-File Report 00-178, 2000.
- TRICART, J. *Ecodinâmica*. 1 ed. Rio de Janeiro: IBGE. 91p. 1977.
- VELOSO, H.P.; RANGEL-FILHO, A.L.R.; LIMA, J.C.A. Classificação da vegetação brasileira, adaptada a um sistema universal. Rio de Janeiro: Fundação Instituto Brasileiro de Geografia e Estatística, 123 p. 1991.
- ZHU, Z.-T.; CAI, F.; CHEN, S.-L.; GU, D.-Q.; FENG, A.-P.; CAO, C.; QI, H.-S.; LEI, G. Coastal Vulnerability to Erosion Using a Multi-Criteria Index: A Case Study of the Xiamen Coast. *Sustainability*, Basiléia, 11, 93. 2019.
- UNDESA – United Nation Department of Economic and Social Affairs. UN Ocean Conference, Fact Sheet: Factsheet: People and Oceans. 2017.

7. ACKNOWLEDGEMENTS

The authors thank the Coordination for the Improvement of Higher Education Personnel (CAPES) and the National Council for Scientific and Technological Development (CNPq) for funding.

Received in: 04/08/2020

Accepted for publication in: 06/08/2021

